• **Basic Research** •

Effect of integrin α5β1 inhibition on SDF-l/CXCR4-mediated choroidal neovascularization

Yang Lyu[1,2], Wen-Qin Xu[1], Li-Juan Sun[1], Xiao-Yan Pan[1], Jian Zhang[3], Yu-Sheng Wang[1]

[1]Department of Ophthalmology, Eye Institute of China PLA, Xijing Hospital, the Fourth Military Medical University, Xi'an 710032, Shaanxi Province, China
[2]Department of Ophthalmology, General Hospital of Lanzhou Military Command, Lanzhou 730050, Gansu Province, China
[3]Department of Biochemistry and Molecular Biology, the Fourth Military Medical University, Xi'an 710032, Shaanxi Province, China

Co-first authors: Yang Lyu and Wen-Qin Xu
Correspondence to: Yu-Sheng Wang. Department of Ophthalmology, Eye Institute of China PLA, Xijing Hospital, the Fourth Military Medical University, Xi'an 710032, Shaanxi Province, China. wangys003@126.com; Jian Zhang. Department of Biochemistry and Molecular Biology, the Fourth Military Medical University, Xi'an 710032, Shaanxi Province, China. biozhangj@hotmail.com

Abstract

● **AIM:** To investigate the roles of integrins in choroidal neovascularization (CNV) and their associations with the stromal cell-derived factor-1 (SDF-1)/CXCR4 axis.
● **METHODS:** CNV lesions were induced in mice using laser photocoagulation. After CNV induction, all animals were randomly assigned to: control, SDF-1, SDF-1+age-related macular degeneration (AMD) 3100 (CXCR4 inhibitor), and SDF-1+ATN161 (integrin α5β1 inhibitor) groups; their effects on CNV progression were observed using hematoxylin eosin (HE) staining, fundus fluorescein angiography (FFA) grading and optical coherence tomography (OCT), and their effects on CXCR4/integrin α5 expression were evaluated using Western blot and double immunofluorescence staining. Hypoxia-exposed endothelial cells (ECs) were used to simulate CNV *in vitro*, they were treated with SDF-1, combined with CXCR4 siRNA/AMD3100 or ATN161, and expression of integrin α5, cell migration and tube formation were analyzed.
● **RESULTS:** Integrin subunit α5 increased at 3rd and 7th day and decreased at 14th day in CNV mice, with no significant change of β1-integrin. CXCR4 expression in CNV mice had persistent increase within 14d after induction. SDF-1 treatment significantly promoted the CNV progression during 3-14d. The mean CNV length in AMD3100 and ATN161 group at day 7 was 270.13 and 264.23 µm in HE images, significantly lower than the mean length in SDF-1 (345.70 µm) group. AMD3100 and ATN161 also significantly reduced thickness and leakage of CNV induced by SDF-1. Mean integrin α5 positive area in SDF-1 group reached $2.31×10^4$ µm², significantly higher than control ($1.25×10^4$ µm²), which decreased to $1.78×10^4$ µm² after AMD3100 treatment. About 61.36% of ECs in CNV lesions expressed α5 in SDF-1 group, which significantly decreased to 43.12% after AMD3100 treatment. *In vitro*, integrin α5 peaked by 6 folds after 6h of hypoxia exposure and CXCR4 gradually increased by up to 2.3 folds after 24h of hypoxia. Approximately 25.12% of ECs expressed integrin α5 after SDF-1 stimulation, which decreased to 7.2%-9.5% after si-CXCR4 or AMD3100 treatment. ATN161 exerted an inhibitory effect comparable to that of si-CXCR4 on EC migration and tube formation in the presence of SDF-1.
● **CONCLUSION:** SDF-1/CXCR4 signaling induces integrin α5β1 expression in ECs to promote CNV.
● **KEYWORDS:** choroidal neovascularization; endothelial cells; stromal cell-derived factor-1; CXCR4; integrin α5β1; hypoxia

INTRODUCTION

Pathological angiogenesis in the eye often leads to serious consequences, including intractable high intraocular pressure, visual impairments, and even irreversible blindness. Choroidal neovascularization (CNV) is a common and devastating disease that causes irreversible vision loss and has emerged as the leading cause of blindness among people aged ≥50y[1]. CNV is characterized by the formation of new blood vessels in the choroid that break through the retinal pigment epithelium (RPE) and Bruch's membrane and grow into the subretinal space, ultimately causing exudative or hemorrhagic retinal detachment[2]. The pathogenesis of CNV involves various genetic or environmental factors and is associated with angiogenesis and vasculogenesis. However, the mechanisms of neovascularization are not completely understood.

Chemokine receptors are a superfamily of G-protein-coupled cell surface receptors. Interactions between chemokine receptors and specific chemokines induce the directional migration of cells toward a gradient of chemokines[3]. CXCR4, in parallel with its unique ligand stromal cell-derived factor-1 (SDF-1), is commonly expressed in CNV and implicated in several types of ocular neovascularization associated with the mobilization, migration and adhesion of endothelial cells (ECs)[4]. However, according to several studies, CXCR4 does not directly contribute to cell adhesion and migration but is essential for transmitting SDF-1-induced signals[5]. Therefore, other mediators may be involved in SDF-1/CXCR4 signaling to promote EC migration and adhesion.

Integrins are heterodimeric receptors containing α and β subunits that function as cell adhesion molecules. Integrin α5β1 is absent or expressed at low levels in healthy ECs but is enriched during embryogenesis, tissue repair, and neovascularization[6]. In the present study, we will elaborate the roles of α5β1 in SDF-1/CXCR4-induced murine CNV and SDF-1/CXCR4-mediated EC migration and tube formation *in vitro*.

MATERIALS AND METHODS

Laser Photocoagulation Induction of CNV in Mice Experimental procedures performed in animals were conducted in accordance with the guidelines of the Animal Ethics Committees of the Fourth Military University and adhered to the ARVO Statement for the Use of Animals in Ophthalmic and Vision Research. Male C57BL/6 mice (aged 6-8wk) were housed in a barrier facility with *ad libitum* access to food and water under a 12h light/dark cycle. Sixty male mice were used in this study.

Laser photocoagulation-induced murine CNV was performed as previously reported[7]. Briefly, the eyes of each animal were exposed to a 532-nm wavelength laser (Twin, Quantel, France) and burns were induced on the fundus 1.5-2 disc diameters from the optic nerve (100 μm, 125 mV and 0.1s). Any laser spots that induced the rupture of Bruch's membrane (confirmed by a vaporization bubble without hemorrhage) were considered effective and CNV lesions available for examination in the present study. After CNV induction, all animals were assigned to the following groups for *in vivo* and *ex vivo* experiments: control, SDF-1 treatment (200 ng/mL; Sino Biological Inc., Beijing, China), SDF-1 (200 ng/mL)+age-related macular degeneration (AMD) 3100 (200 mmol/L) treatment (Selleckchem, Houston, USA), and SDF-1 (200 ng/mL)+ATN161 (2 mg/mL; TOCRIS, Bristol, UK) treatment. All agents were dissolved in phosphate buffer solution (PBS) at the indicated doses and injected (1 μL) at a single dose into the posterior vitreous cavity; their effects were observed for 3, 7 and 14 consecutive days.

Cell Culture Rhesus macaque choroid-retinal ECs (RF/6A) and RPE cells were obtained from the Chinese Academy of Science (Shanghai, China) and routinely cultured in Dulbecco's modified Eagle's medium (DMEM; Invitrogen, CA, USA) containing 15% fetal bovine serum (FBS; Invitrogen), 100 U/mL penicillin, and 100 μg/mL streptomycin in a humidified atmosphere with 5% CO_2 at 37℃. ECs were exposed to atmosphere comprising a mixture of 5% CO_2, 1% O_2 and 94% N_2 at 37℃ to induce hypoxia. The same final concentrations of SDF-1, AMD3100 and ATN161 used in the animal study were also used in the cell-based experiments.

Antibodies We used the following antibodies against αv/β3/β5/α5/β1: rabbit monoclonal antibodies (used for Western blot double labeling) against αv (Abcam, Cambridge, UK, 179475), β3 (Abcam, 119992), β5 (Cell Signaling Technology, MA, USA, D24A5), α5 (Abcam, 150361), and β1 (Abcam, 179471). We also used a goat polyclonal antibody against CXCR4 (Abcam, 1670). The following rat monoclonal antibodies were used for double immunofluorescence staining: α5 (Abcam, 150361), CXCR4 (Abcam, 1670), and CD31 (Abcam, 28364). An α5 antibody (Abcam, 150361) was used for flow cytometry. Antibodies against β-actin were obtained from Santa Cruz Biotechnology (CA, USA). Recombinant human secondary antibodies, including goat anti-rabbit conjugated to Alexa Fluor 594/CY3 or Alexa Fluor 488/FITC, were purchased from Beijing ComWin (Beijing, China).

Hematoxylin Eosin Staining The histopathological analysis of CNV severity in animals exposed to various treatments was performed using previously reported methods (3 eyes in each group, 4-6 spots per eye)[7]. Anesthetized mice were transcardially perfused with 0.9% saline followed by 4% paraformaldehyde. Paraffin-embedded tissues were serially sectioned at 3 mm and stained with hematoxylin eosin (HE). Serial sections of each CNV sample were examined and digital images were captured under a light microscope (BX51, Olympus Corporation, Tokyo, Japan). The CNV thickness was determined in vertical sections by measuring the distance from the adjacent RPE layer to the top of the CNV. The CNV length was identified as the maximum horizontal distance of the CNV lesion using Image-Pro Plus (IPP) 6.0 software.

Optical Coherence Tomography Optical coherence tomography[8] (OCT) "TruTrack TM Active Eye Tracking" and "Automatic RealTime (ART)" technologies were used, and follow-up images were derived from the same lesion, which eliminated the subjective placement of the scan by the operator. The CNV thickness was quantified using software provided by OptoProbe Research Ltd. (Burnaby, BC, Canada). Four to six spots from lesions in each eye were selected for follow-up and analysis. A CNV lesion was defined by the presence of spindle-shaped, subretinal, hyperreflective material above the RPE layer. The B-scan passing through the "geometric" lesion center was chosen for analysis to evaluate the thickness of each tracked CNV lesion.

Fundus Fluorescein Angiography Fundus fluorescein angiography (FFA) images were captured under a confocal scanning laser ophthalmoscope (OptoProbe Research Ltd., Burnaby, BC, Canada), immediately followed by OCT. Briefly, the three groups of mice were evaluated on the 7th day after CNV induction; the mice were anesthetized and intraperitoneally injected with 0.1 mL of 2.5% sodium fluorescein (Wuzhou Pharmaceutical, Guangxi, China). FFA images were recorded using a digital imaging system (Heidelberg Engineering). A blinded assessment of fluorescein angiogram images was conducted by two retinal specialists. Fluorescein leakage intensity was graded as follows: 0, no leakage; 1, slight leakage; 2, moderate leakage; 3, prominent leakage.

Choroidal Flatmount Seven days after CNV induction, mice were anesthetized with sodium pentobarbital and perfused with PBS through the left cardiac ventricle, followed by perfusion with 4% paraformaldehyde. After sacrifice, the eyes of each animal were enucleated and fixed with chilled 4% paraformaldehyde in 0.1 mol/L phosphate buffer (PB) for 2h. Next, the anterior segment and vitreous were resected; the remaining RPE-choroid-sclera complex was flatmounted with six or more radial cuts and permeabilized with 0.2% Triton X-100 for 24h. Afterwards, the flatmounts were transferred and cultured in rhodamine-conjugated *Ricinus communis* agglutinin (1:1000; Vector Laboratories, Burlingame, CA, USA) for 24h. The flatmounts were then washed with 0.01 mol/L Tris buffered saline-Tween (TBST) for 24h, incubated with anti-α5 or CXCR4 antibodies at 4℃ for 18 to 20h, washed with PBS, stained with lectin (1:100) overnight at 4℃ overnight, and washed with PBS three times after mounting. Images of the flatmounts were captured using a confocal laser scanning microscope (FV1000, Olympus Corporation, Tokyo, Japan), and the CNV area was calculated using IPP 6.0 software.

Immunofluorescence Staining Seven days after treatment, mice were anesthetized with sodium pentobarbital and sequentially perfused with PBS and 4% paraformaldehyde through the left cardiac ventricle. After sacrifice, the eyes of each animal were enucleated and fixed with chilled 4% paraformaldehyde in 0.1 mol/L PB for 2h. Then, the anterior segment and vitreous were resected, and the posterior eyecups were cryoprotected in graded sucrose solutions (20% and 30% in PB). The eyecups were embedded, sectioned vertically at an 8-μm thickness, permeabilized for 10min, blocked for 30min, and incubated with primary antibodies overnight at 4℃. Then, the sections were incubated with combinations of secondary antibodies for 1h and stained with diamino-2-phenyl-indol (DAPI). Immunofluorescence staining was visualized using a confocal microscope.

Western Blot Tissue or cell lysates were prepared in lysis buffer [50 nmol/L Tris-HCl, 150 nmol/L NaCl, 1% Nonidet P-40 (NP40), 0.1% sodium dodecyl sulfate (SDS), 0.5%

deoxycholate, and 1 mmol/L phenylmethylsulfonyl fluoride], and protein concentrations were determined using a BCA protein assay kit (Sangon Biotech, Shanghai, China). Equal amounts (20 μg) of protein were electrophoresed on a 10% SDS polyacrylamide gel and transferred to a polyvinylidene fluoride (PVDF) membrane (Millipore, MA, USA). Primary antibodies incubated with the membranes overnight at 4℃. Membranes were incubated with secondary antibodies for 30min. After three washes with TBST, signals from the protein band were detected with an enhanced chemiluminescence system (Millipore) and standardized to β-actin levels.

RNA Interference RF/6A cells were seeded at a density of 1.0×10^4 cells/well in six-well plates and grown to 70%-80% confluence before transfection. Transfections of small interfering RNAs (siRNAs) or negative controls were performed using Lipofectamine 2000 from Invitrogen (Carlsbad, CA, USA), according to the manufacturer's instructions. The sequences of the synthesized siRNAs were as follows: CXCR4 (CXCR4-612: sense 5'-3'GGGUGGUUGUGUUCCAGUUTT, antisense 5'-3'AACUGGAACACAACCACCCTT; CXCR4-1083: sense 5'-3'GCCUCAAGAUCCUUUCCAATT, antisense 5'-3'UUGGAAAGGAUCUUGAGGCTT; CXCR4-163: sense 5'-3'CCAUGAAGGAACCCUGUUUTT, antisense 5'-3'AAACAGGGUUCCUUCAUGGTT); and negative control siRNA (sense 5'-3'UUCUCCGAACGUGUCACGUTT, antisense 5'-3'ACGUGACACGUUCGGAGAATT). For all experiments, the cells were transfected with siRNAs 48h before further treatments.

Enzyme-linked Immunosorbent Assay Cells were incubated under hypoxic conditions, and media were collected at the indicated times. The level of the SDF-1 protein secreted by RPE cells into the culture medium was measured using an enzyme-linked immunosorbent assay (ELISA) kit (JingMei Biotech, Shenzhen, China) according to the manufacturer's instructions. Representative results were obtained from three independent experiments and are expressed in pg/mL.

Quantitative Real-time Polymerase Chain Reaction Total RNA was extracted from choroidal tissue, RF/6A cells or RPE cells using TRIzol reagent (Invitrogen), according to the manufacturer's instructions. The cDNA templates were prepared using a reverse transcription (RT) system (TaKaRa Dalian, Dalian, China). Polymerase chain reaction (PCR) was performed in triplicate using a kit (SYBR Premix EX Taq; TaKaRa) and an ABI PRISM 7500 Real-time PCR System, with β-actin serving as an internal control. The PCR primers were: SDF-1: sense 5'-3'GATTGTAGCCCGGCTGAAGA and antisense 5'-3'TTCGGGTCAATGCACACTTGT; and CXCR4-monkey-354: sense 5'-3'GCAAGGCAGUCCAUGUCAUTT and antisense 5'-3'AUGACAUGGACUGCCUUGCTT.

Flow Cytometry A fluorescence-activated cell sorter (FACS) analysis was performed using a FACSCalibur™ flow cytometer (BD Immunocytometry Systems). Data were analyzed using FlowJo vX.0.6 software (FlowJo, LLC, Ashland, OR, USA).

***In Vitro* Tube Formation Assay** Matrigel Basement Membrane Matrix (BD Biosciences) was thawed overnight at 4℃, diluted with medium, and used to coat the wells of 48-well plates at 37℃ for 40min. RF/6A ECs (2×10^5) were seeded onto the gel in 400 μL of medium and incubated at 37℃ in a 5% CO_2 atmosphere for 26h. The length of the tubes was measured using IPP software, and the results are expressed as the mean fold change in tube length compared with the length of the control group. For each experiment, cells were seeded into at least three wells per condition, and each experiment was repeated three times.

Endothelial Cell Migration Assay All migration assays were assessed in a 24-well modified Boyden chamber (Corning, NY, USA) in which the two compartments were separated by a polycarbonate filter with a pore size of 8 mm. Briefly, 200 μL of RF/6A cells in serum-free medium (1×10^4 cells/mL) were seeded in the upper chamber, and negative control cells suspended in the same medium were added to the bottom chamber to a final volume of 500 μL. The chambers were incubated at 37℃ in a 5% CO_2 atmosphere for 24h. Migrated cells were fixed with 4% paraformaldehyde for 10min and stained with 1% crystal violet in methanol. The number of migrated cells was counted under a fluorescence microscope. Five randomly chosen fields from each insert were counted, and values were averaged. Each experiment was performed in triplicate.

Statistical Analysis Statistical analyses were conducted using SPSS 22.0 software. Data are presented as means±SD. Comparisons between two groups were performed using Student's *t*-test. Analysis of variance followed by the least significant difference (LSD) test were used for multiple comparisons. Chi-square tests were used to compare categorical data. Statistically significant differences were indicated when two-tailed *P* values were less than 0.05.

RESULTS

Expression of SDF-1/CXCR4 and Integrin Subunits in CNV Tissues and Cells Cultured Under Hypoxic Conditions
We established hypoxia-exposed RPE cells or ECs *in vitro* and in mice with laser-induced CNV to evaluate whether SDF-1/CXCR4 and integrins participated in CNV. SDF-1 expression gradually increased over time in the RPE cells cultured under hypoxic conditions and peaked after 24h of hypoxia. The expression of the SDF-1 mRNA peaked after 6h of hypoxia (Figure 1A). Additionally, we evaluated the expression of CXCR4 and integrin subunits in Rhesus macaque choroid-retinal ECs (RF/6A) during hypoxia. Levels of the CXCR4 protein increased over time in ECs cultured under hypoxic conditions and peaked after 24h of hypoxia. The expression of the CXCR4 mRNA initially increased and peaked at 12h, but then decreased during the observation (Figure 1B). Next, we measured the expression of various integrin subunits after 0, 6, 12 and 24h of hypoxia. No significant differences in integrin αv and β1 expression were observed during hypoxia. Integrin β3, β5, and α5 expression initially increased and then decreased; the highest expression and greatest changes in the levels of these proteins were observed after 6h of hypoxia (Figure 1C).

We also determined the expression of integrins and CXCR4 in mice with laser-induced CNV after 3, 7 and 14d using Western blotting. No significant differences in integrin αv and β1 expression were observed in CNV mice. Integrin β3, β5 and α5 expression appeared to increase and then decrease during the progression of CNV; their expression levels were highest exhibited marked changes after 7d. CXCR4 expression increased over the course of CNV and the highest levels were observed 14d after CNV induction (Figure 2). Integrin β3, β5 and α5 and CXCR4 expression showed an increasing trend in response to hypoxia and CNV induction. In the present study, we focused on the role of integrin α5β1 in CNV.

SDF-1 Increases the Severity of CNV in Laser-induced Mice *via* the CXCR4 Receptor In the vertical view of cross sections, neither SDF-1 stimulation nor subsequent CXCR4 inhibition significantly affected the CNV thickness in laser-insulted animals on the indicated days, as determined by HE staining (Figure 3A-3C). The CNV length gradually increased and peaked at 7d after CNV in each group. At each time point, a significant increase in the CNV length was detected after SDF-1 treatment compared with that in the control treatment. The CNV length was substantially decreased after CXCR4 blockade using AMD3100. The changes in the laser-induced CNV *in vivo* were also examined using OCT at 3, 7 and 14d in each group. OCT images revealed that the CNV lesions exhibited a hyperreflective outline and hyporeflective cavity. Following laser exposure, a subretinal, spindle-shaped hyperreflective area was observed. The outline of the laser-induced lesion was less reflective in OCT images captured on day 3, reached its maximum size on day 7, and was blurred on day 14. Notably, on day 7, the maximum height of the RPE layer was observed, and the thickness of the RPE layer in the SDF-1 group was substantially increased compared with that in control animals. CXCR4 inhibition substantially reduced the SDF-1-induced increase in the thickness of the RPE layer in OCT images (Figure 3D-3E).

CNV activity evaluations were performed using FFA. The laser spots exhibited a large hyperfluorescent core surrounded by a lace-like boundary on day 7 in control mice. Compared with CNV lesions in the control group, CNV lesions in the SDF-1-treated group showed obvious fluorescence leakage
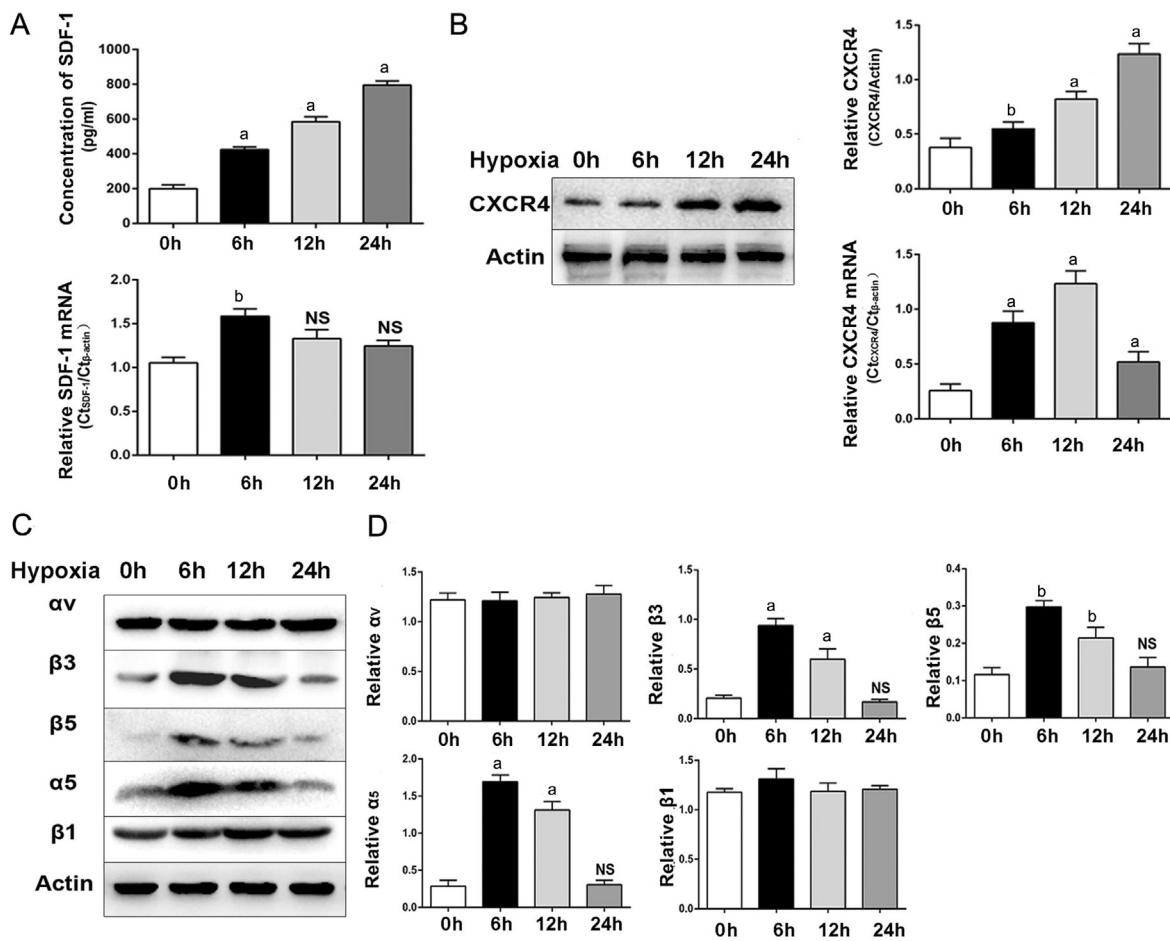
Figure 1 Profiles of SDF-1/CXCR4 and integrin expression in hypoxia-exposed RPE or RF/6A cells A: ELISA and qRT-PCR analysis of SDF-1 levels in hypoxia-stimulated RPE cells at the indicated time points; B: Western blot and qRT-PCR analyses of CXCR4 expression in hypoxia-exposed RF/6A cells; C: Western blot and quantitative analyses (D) of the levels of integrin subunits and CXCR4 in RF/6A cells cultured under hypoxic conditions for the indicated times. [a]$P<0.01$; [b]$P<0.05$; NS: $P>0.05$ compared with the control group.
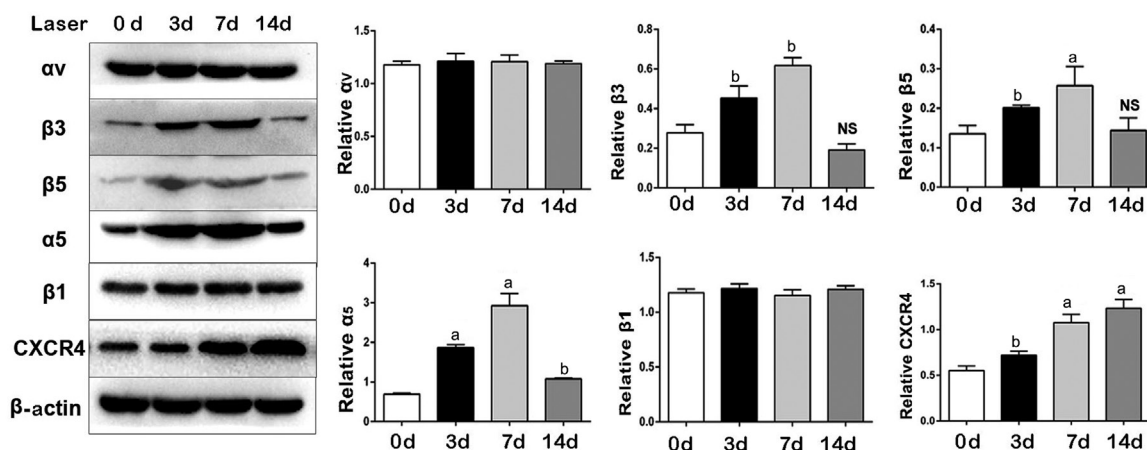
Figure 2 Profiles of SDF-1/CXCR4 and integrin expression in mice with laser-induced CNV Western blot and quantitative analyses of the levels of integrin subunits and CXCR4 in mice with laser-induced CNV at the indicated times. $n=3$, [a]$P<0.01$; [b]$P<0.05$; NS: $P>0.05$ compared with the control group.

with a large and diffuse area, as well as a higher ratio of grades 2 and 3 CNV leakage. However, no difference in fluorescence leakage was observed between the SDF-1 group and SDF-1+AMD3100 group (Figure 3F-3G). Flatmount examinations revealed a larger CNV area and volume in the SDF-1-stimulated group than in the control group. The addition of

AMD3100 significantly suppressed the increase in CNV area and volume induced by SDF-1 (Figure 3H-3J).

SDF-1 Increases CXCR4 and α5 Expression in CNV Mice We confirmed that the SDF-1 group exhibited increased α5 and CXCR4 expression in the CNV region. The α5- and CXCR4-positive areas of the CNV lesions were significantly
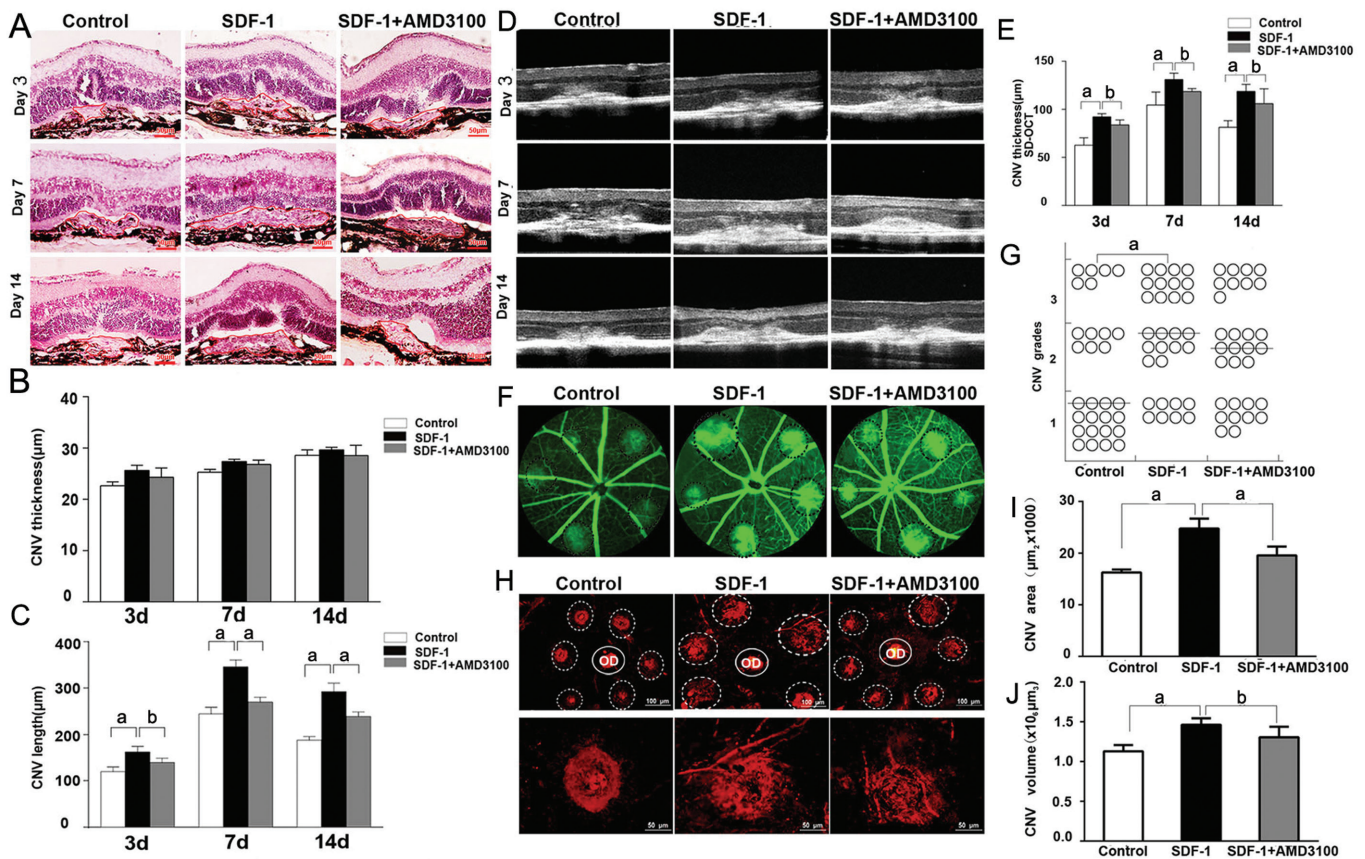
Figure 3 SDF-1/CXCR4 signaling promotes laser-induced CNV in mice CNV was induced in animals using laser photocoagulation, followed by SDF-1 and SDF-1+AMD3100 injections on the indicated days. A-C: HE staining of CNV lesions and quantification of the CNV thickness and length in cross sections from the three groups. The margins of the CNV lesion are outlined by solid red lines. Scale bar, 50 μm; D-E: Representative OCT images and results of the analysis of CNV thickness using OCT in laser-treated mice; FFA imaging (F) and CNV grading (G) of the three groups on day 7. CNV lesions are circled by dashed black lines (the line represents the median of each group); H: Representative CNV areas in choroidal flatmounts from the indicated groups. Blood vessels in choroidal flatmounts were stained with rhodamine-conjugated agglutinin. A CNV lesion (dashed line) formed around the optic disc (solid line). Scale bar, 100 μm. Magnified image of a single CNV lesion. Scale bar, 50 μm; I-J: CNV areas and volumes were quantified in laser-induced mice. n=6; [a]P<0.01, [b]P<0.05.

increased on day 7 after SDF-1 treatment compared with those in the control treatment, paralleling the increase in α5/CNV and CXCR4/CNV area ratios. However, CXCR4 blockade using AMD3100 exerted a significant inhibitory effect on α5/CXCR4-positive areas, as well as α5/CNV and CXCR4/CNV area ratios (Figure 4).

Additionally, we observed the effect of SDF-1 on α5 and CXCR4 expression in ECs using double-immunofluorescence staining with a CD31 antibody. The number of α5- and CXCR4-positive ECs was counted in the laser spots of CNV cross sections. The numbers of α5- or CXCR4-positive cells and α5/CNV- or CXCR4/CNV-labeled cells in the SDF-1 group were significantly increased, but were substantially decreased after CXCR4 inhibition (Figure 5).

SDF-1/CXCR4 Upregulates Integrin α5 Expression in Choroidal Endothelial Cells We silenced CXCR4 using siRNAs to determine whether integrin α5 expression was controlled by SDF-1/CXCR4 signaling. We transfected RF/6A cells with a combination of three different siRNA sequences (each at a 1/3 dose) to achieve optimal silencing efficiency

(Figure 6A). The expression of integrin α5 in the SDF-1 group was significantly elevatedcompared with that in the control (P<0.05). However, pharmacological or genetic CXCR4 inhibition significantly suppressed the level of integrin α5 observed in response to SDF-1 stimulation (Figure 6B). In addition, the percentage of α5 integrin-positive cells after each treatment was consistent with the results obtained using Western blotting (Figure 6C).

Integrin α5 Mediates SDF-1/CXCR4-induced EC Migration and Tube Formation RF/6A cells gradually formed tubular structures after treatment with SDF-1. Notably, compared with the control, SDF-1 significantly increased lumen formation at 20h (Figure 7A). A decrease in lumen formation was observed after CXCR4 inhibition or α5 integrin inhibition using ATN161, despite the presence of SDF-1. Moreover, the addition of CXCR4 functional inhibitors and specific siRNAs, as well as ATN161, inhibited retinal EC angiogenesis (Figure 7B). A markedly greater number of migrated cells was observed in the SDF-1 group than in the control group (P<0.05). After treatment with SDF-1+AMD3100, SDF-1+si-CXCR4 and
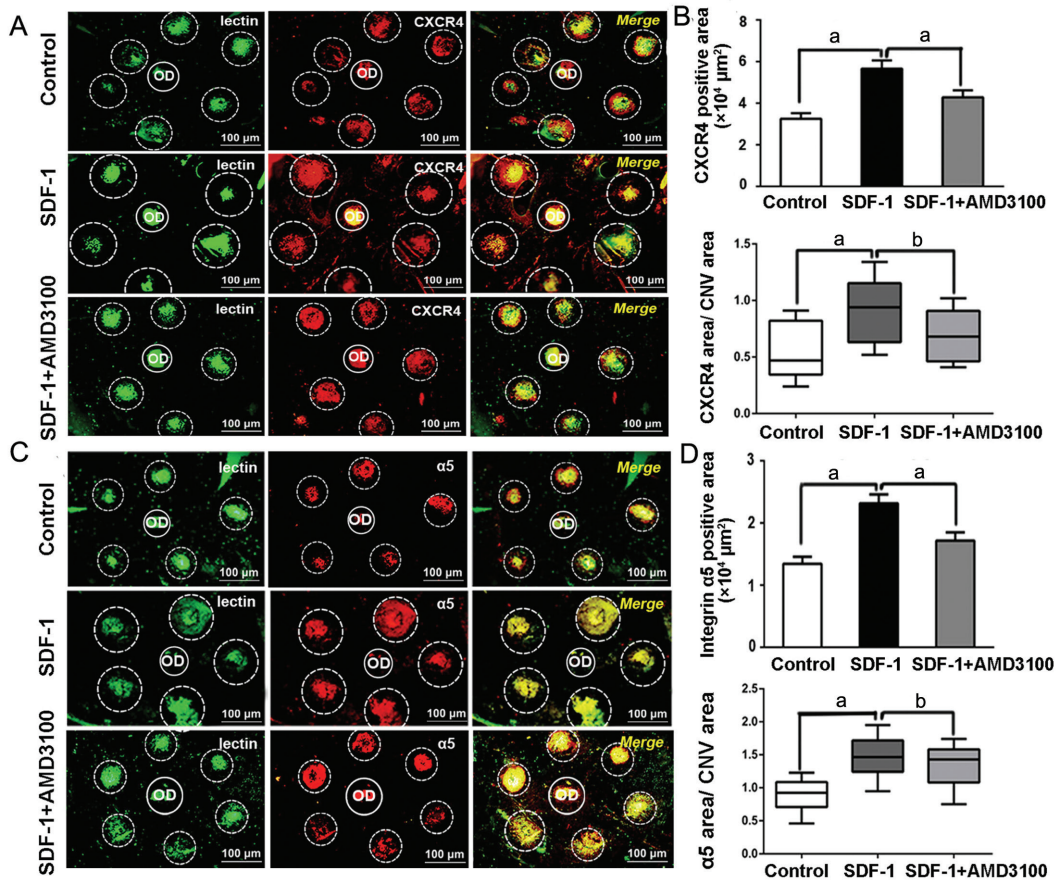
Figure 4 Expression of integrin α5 and CXCR4 in CNV mice CNV was induced in animals using laser photocoagulation, followed by SDF-1 and SDF-1+AMD3100 injections on day 7. Representative images of choroidal flatmounts (A, C) and quantification of the α5- and CXCR4-expressing areas and ratios in CNV lesions (B, D) after laser induction. CNV lesions (dashed line) formed around the optic disc (solid line). Scale bar, 100 μm. n=6; [a]P<0.01, [b]P<0.05.
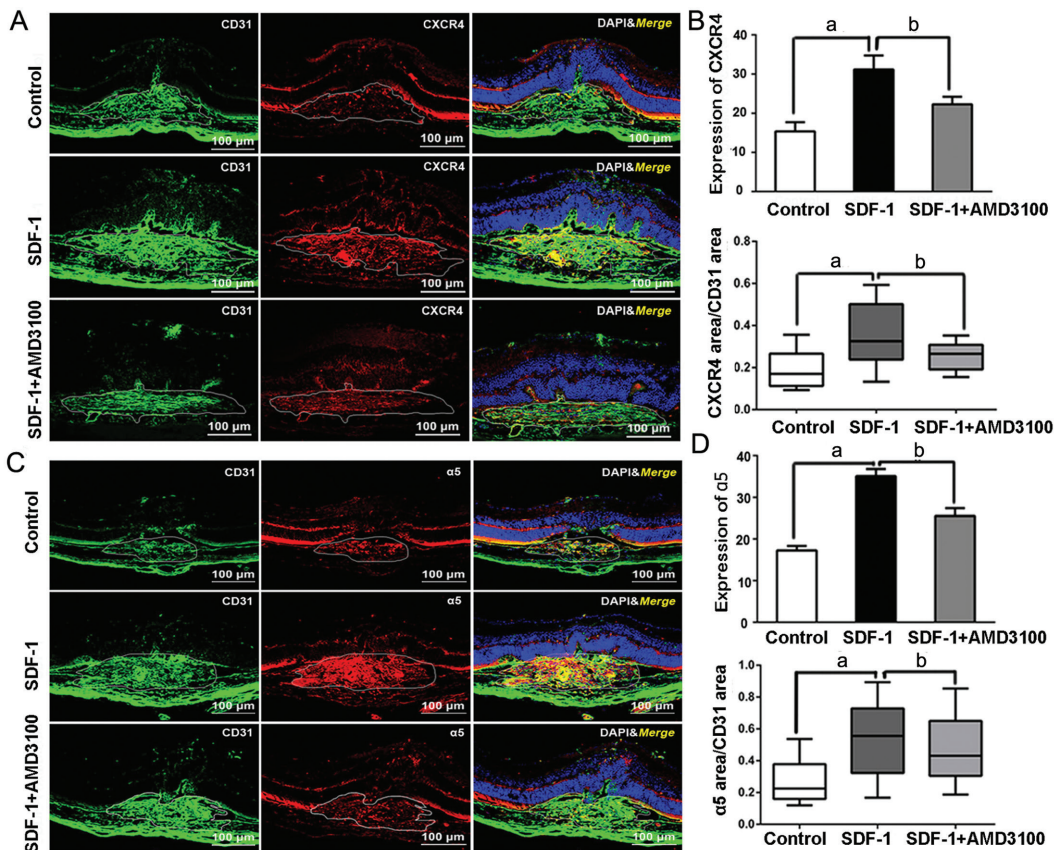
Figure 5 Expression of integrin α5 and CXCR4 in ECs from CNV mice CNV was induced in animals using laser photocoagulation, followed by SDF-1 and SDF-1+AMD3100 injections on day 7. Representative confocal images of the CNV lesion areas in different groups on day 7 (A, C) and quantification of α5 and CXCR4 expression relative to CD31 (B, D). Scale bar, 100 μm. n=6; [a]P<0.01, [b]P<0.05.
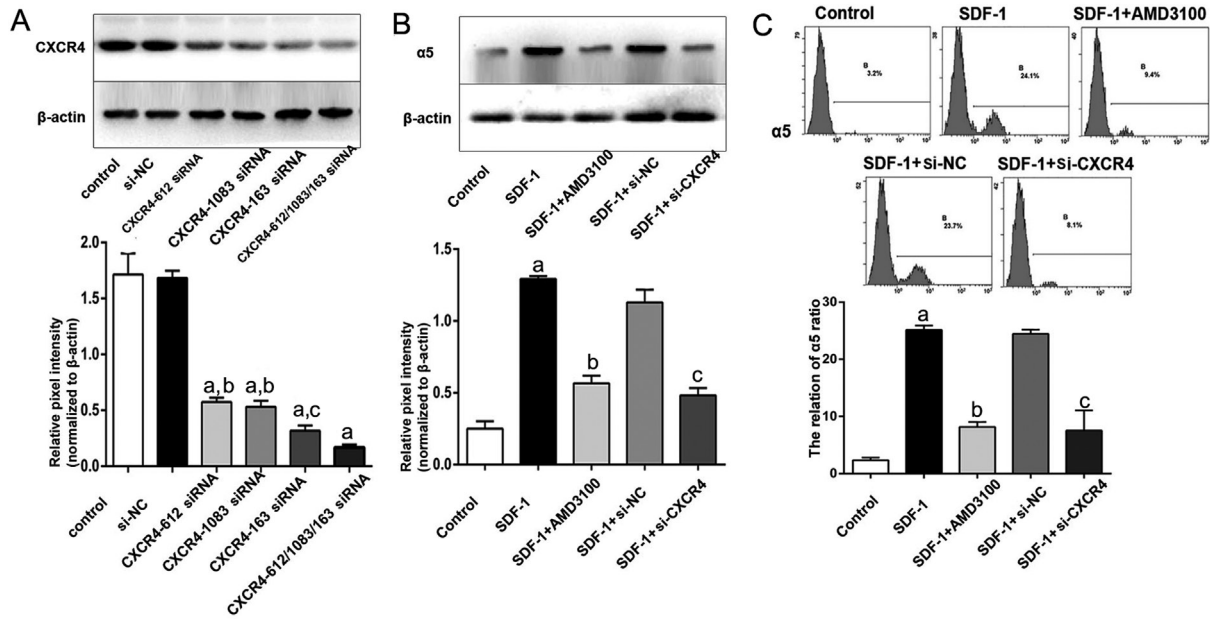
Figure 6 Effects of SDF-1/CXCR4 signaling on integrin α5 expression on ECs A: Inhibitory effect of the CXCR4 siRNA on CXCR4 expression in RF/6A cells. [a]P<0.01 compared with the si-NC group; [b]P<0.01, [c]P<0.05 compared with the group transfected with the three siRNA sequences. Integrin α5 expression (B) and flow cytometry analysis of the percentage of α5-positive RF/6A cells (C) after CXCR4 inhibition in the presence of SDF-1, [a]P<0.05 compared with the control, [b]P<0.05 compared with the SDF-1 group, [c]P<0.05 compared with the SDF-1+si-NC group.
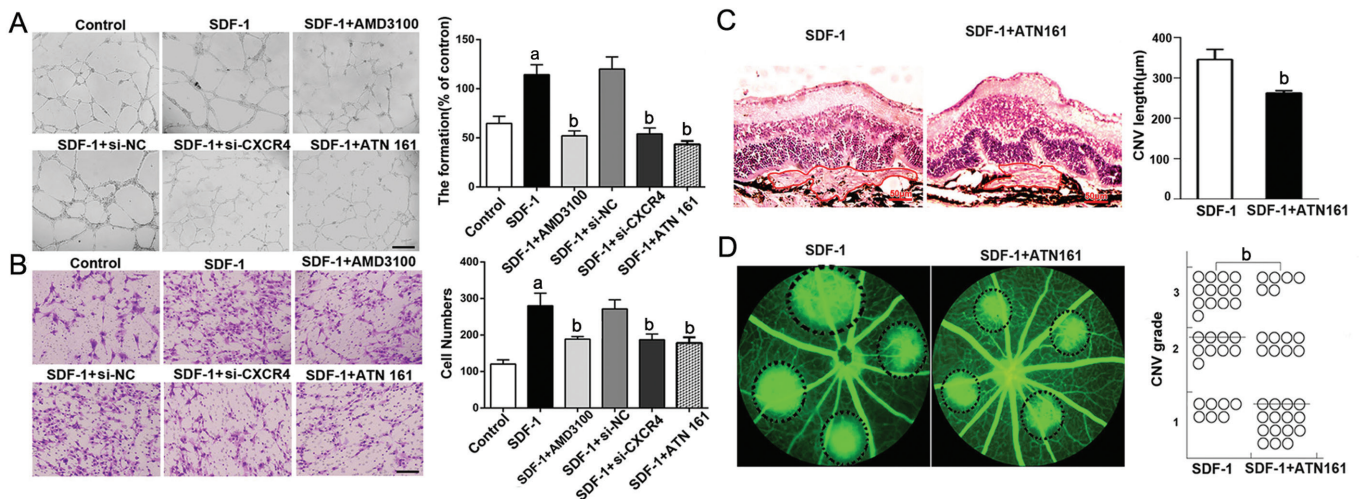
Figure 7 Effects of SDF-1/CXCR4 and integrin α5 on EC migration and tube formation A: Tube formation of RF/6A cells in response to SDF-1 induction and CXCR4 inhibition or integrin α5β1 inhibition using ATN161 (2 mg/mL), scale bar, 500 μm; B: Transwell assay of RF/6A cell migration, scale bar, 500 μm; C: HE staining of CNV lesions and quantification of the CNV length in cross sections from the two groups on day 7; D: Fundus fluorescence angiography imaging of the two groups on day 7. n=6; [a]P<0.05 compared with the control, [b]P<0.05 compared with the SDF-1 group.

SDF-1+ATN161, a marked decrease in the number of migrated cells was observed. Furthermore, the injection of ATN161 in mice greatly reduced the CNV length and leakage areas induced by SDF-1 (Figure 7C-7D).

DISCUSSION

Choroidal neovascularization represents an important pathological cause of intractable and severe vision loss in approximately 40 ocular diseases; the most common of these diseases is AMD[9]. Neovascularization is induced by several factors, such as ischemia, hypoxia or inflammation[10-11]. Newly constructed vessels are always structurally fragile and prone to hemorrhage, thus leading to edema, exudates and accompanying fibrosis[12]. Therefore, the suppression of neovascularization plays a pivotal role in the treatment of choroidal lesion-related ocular diseases. Inhibition of SDF-1/CXCR4 signaling and subsequent integrin α5β1 expression substantially suppressed CNV lesions in mice, as well as the migration and tube formation of ECs in the present study. Agents targeting this signaling pathway could become an alternative treatment option for CNV.

Pathological changes observed in CNV lesions involve various cells, cytokines and signaling cascades. Basically, after

sensing complex signal inputs from other cells or cytokines, such as vascular endothelial growth factor (VEGF), tumor necrosis factor (TNF) or SDF-1, naïve or bone marrow-derived cell (BMC)-derived ECs participate in CNV formation *via* proliferation, differentiation, recruitment or migration. Our study focused on the role and mechanism of SDF-1 in CNV, with the objective of providing evidence for potential treatments for AMD beyond targeting VEGF. VEGF is involved in the early steps of angiogenesis, but treatments designed to inhibit VEGF are successful in <50% of patients with neovascular AMD[13-14]. VEGF and SDF-1 were co-localized in RPE cells from surgically excised CNV lesions. VEGF and SDF-1 may also exert synergistic effects on the development of diabetic retinopathy. SDF-1 promotesVEGF production, whereas VEGF enhances the response of ECs to SDF-1[15-16]. Cai *et al*[15] confirmed that SDF-1 is able and sufficient to promote endothelial chemotaxis to the ischemic retina and participate in retinal neovascularization in laser-induced mice. Therefore, we postulated that the inhibition of SDF-1 signaling may also counteract the effect of VEGF on inducing angiogenesis. Zhang *et al*[4] reported that hypoxia-specific hypoxia-inducible factor (HIF)-1α also contributed to the induction of SDF-1 in RPE cells, which shared a similar pattern of HIF-1α on the induction of VEGF. We also detected high level of SDF-1 in RPE cells cultured under hypoxic conditions. However, further studies examining the synergistic effects of SDF-1 and VEGF are required.

In parallel with SDF-1 upregulation, its unique receptor, CXCR4, was elevated in CNV lesions and hypoxia-exposed ECs. The interaction between SDF-1 and CXCR4 regulates the entire process of endothelial mobilization, targeted migration, recruitment and differentiation. SDF-1 also promotes the migration of embryonic stem cell-derived ECs and the formation of the vascular network. The directional migration of ECs shares many similarities with the homing of leukocytes to inflammation sites. As a major chemokine receptor expressed on ECs, CXCR4 induces cell chemotaxis toward a gradient of SDF-1. Furthermore, high levels of SDF-1 have been detected in the retina and choroid, and the SDF-1/CXCR4 axis may function as a "navigation system" for ECs[17-18]. SDF-1/CXCR4 signaling itself is not directly involved in cell adhesion and migration but may be involved by transducing signals to cells *via* other molecules[19]. Therefore, we intended to evaluate the roles of adhesion molecules in the SDF-1/CXCR4 signaling pathway.

Integrins are cell surface adhesion molecules that not expressed in mature ocular blood vessels but selectively expressed in activated ECs. Levels of integrin subunits α5, β3 and β5, but not αv and β1, were increased in both CNV animals and hypoxia-exposed ECs, and their altered expression patterns

were similar to that of CXCR4. Integrin αvβ3 has been detected in CNV membranes in patients with AMD[20]. Patients with diabetic retinopathy and retinal neovascularization present pre-retinal membrane expression of integrins αvβ3 and αvβ5[20]. According to the study by Reynolds and colleagues[21], β3 or β5 integrin knockout mice still form new blood vessels. Therefore, we focused on the roles of integrin α5 in CNV in our study. Integrin α5 was closely associated with CNV and CXCR4 expression. SDF-1 increased integrin α5 subunit expression and the number of integrin α5-positive ECs in CNV lesions, and these effects were reversed by CXCR4 inhibition. In addition, we observed an inhibitory effect of integrin α5β1 suppression on the migration and tube formation of ECs. Integrin α5 mediates the adhesion of cells to the extracellular matrix by binding to fibronectin, which may facilitate the formation of EC tubes following recruitment by SDF-1/CXCR4 signaling. Our findings provide a link between a chemokine receptor and integrins in CNV pathogenesis. Similarly, the association between SDF-1/CXCR4 and adhesion molecules has been described in renal and prostate cancer cells[22]. However, the potential induction mechanism has not been elucidated and requires further research.

Above all, inhibition of CXCR4 or integrin α5β1 substantially suppressed the migration and tube formation of ECs in this study, ultimately reducing lesion areas and leakage of CNV.

ACKNOWLEDGEMENTS

REFERENCES

1 Gao X, Wang Y, Hou HY, Lyu Y, Wang HY, Yao LB, Zhang J, Cao F, Wang YS. In vivo bioluminescence imaging of hyperglycemia exacerbating stem cells on choroidal neovascularization in mice. *Int J Ophthalmol* 2016;9(4): 519-527.

2 Yu YJ, Mo B, Liu L, Yue YK, Yue CL, Liu W. Inhibition of choroidal neovascularization by lentivirus-mediated PEDF gene transfer in rats. *Int J Ophthalmol* 2016;9(8):1112-1120.

3 Zeng Y, Wang X, Yin B, Xia G, Shen Z, Gu W, Wu M. Role of the stromal cell derived factor-1/CXC chemokine receptor 4 axis in the invasion and metastasis of lung cancer and mechanism. *J Thorac Dis* 2017;9(12): 4947-4959.

4 Zhang ZX, Wang YS, Shi YY, Hou HY, Zhang C, Cai Y, Dou GR, Yao LB, Li FY. Hypoxia specific SDF-1 expression by retinal pigment epithelium initiates bone marrow-derived cells to participate in choroidal neovascularization in a laser-induced mouse model. *Curr Eye Res* 2011;36(9):838-849.

5 Feng L, Ju M, Lee KYV, Mackey A, Evangelista M, Iwata D, Adamson P, Lashkari K, Foxton R, Shima D, Ng YS. A proinflammatory function

of toll-like receptor 2 in the retinal pigment epithelium as a novel target for reducing choroidal neovascularization in age-related macular degeneration. *Am J Pathol* 2017;187(10):2208-2221.

6 Wang WQ, Wang FH, Qin WX, Liu HY, Lu B, Chung C, Zhu J, Gu Q, Shi W, Wen C, Wu F, Zhang K, Sun XD. Joint antiangiogenic effect of ATN-161 and anti-VEGF antibody in a rat model of early wet age-related macular degeneration. *Mol Pharm* 2016;13(9):2881-2890.

7 Shi YY, Wang YS, Zhang ZX, Cai Y, Zhou J, Hou HY, van Rooijen N. Monocyte/macrophages promote vasculogenesis in choroidal neovascularization in mice by stimulating SDF-1 expression in RPE cells. *Graefes Arch Clin Exp Ophthalmol* 2011;249(11):1667-1679.

8 Liu T, Hui L, Wang YS, Guo JQ, Li R, Su JB, Chen JK, Xin XM, Li WH. In-vivo investigation of laser-induced choroidal neovascularization in rat using spectral-domain optical coherence tomography (SD-OCT). *Graefes Arch Clin Exp Ophthalmol* 2013;251(5):1293-1301.

9 Gao F, Hou H, Liang H, Weinreb RN, Wang H, Wang Y. Bone marrow-derived cells in ocular neovascularization: contribution and mechanisms. *Angiogenesis* 2016;19(2):107-118.

10 Cabral T, Mello LGM, Lima LH, Polido J, Regatieri CV, Belfort R Jr, Mahajan VB. Retinal and choroidal angiogenesis: a review of new targets. *Int J Retina Vitreous* 2017;3:31.

11 Zhao M, Xie W, Tsai SH, Hein TW, Rocke BA, Kuo L, Rosa RH Jr. Intravitreal stanniocalcin-1 enhances new blood vessel growth in a rat model of laser-induced choroidal neovascularization. *Invest Ophthalmol Vis Sci* 2018;59(2):1125-1133.

12 Xu D, Davila JP, Rahimi M, Rebhun CB, Alibhai AY, Waheed NK, Sarraf D. Long-term progression of type 1 neovascularization in age-related macular degeneration using optical coherence tomography angiography. *Am J Ophthalmol* 2018;187:10-20.

13 Wang H, Fotheringham L, Wittchen ES, Hartnett ME. Rap1 gtpase inhibits tumor necrosis factor-alpha-induced choroidal endothelial migration via NADPH oxidase- and NF-kappab-dependent activation of rac1. *Am J Pathol* 2015;185(12):3316-3325.

14 Sato T, Takeuchi M, Karasawa Y, Enoki T, Ito M. Intraocular inflammatory cytokines in patients with neovascular age-related macular degeneration before and after initiation of intravitreal injection of anti-VEGF inhibitor. *Sci Rep* 2018;8(1):1098.

15 Cai Y, Li X, Wang YS, Shi YY, Ye Z, Yang GD, Dou GR, Hou HY, Yang N, Cao XR, Lu ZF. Hyperglycemia promotes vasculogenesis in choroidal neovascularization in diabetic mice by stimulating VEGF and SDF-1 expression in retinal pigment epithelial cells. *Exp Eye Res* 2014;123:87-96.

16 Grierson R, Meyer-Rusenberg B, Kunst F, Berna MJ, Richard G, Thill M. Endothelial progenitor cells and plasma vascular endothelial growth factor and stromal cell-derived factor-1 during ranibizumab treatment for neovascular age-related macular degeneration. *J Ocul Pharmacol Ther* 2013;29(6):530-538.

17 Maddirela DR, Kesanakurti D, Gujrati M, Rao JS. MMP-2 suppression abrogates irradiation-induced microtubule formation in endothelial cells by inhibiting alphavbeta3-mediated SDF-1/CXCR4 signaling. *Int J Oncol* 2013;42(4):1279-1288.

18 Feng YF, Guo H, Yuan F, Shen MQ. Lipopolysaccharide promotes choroidal neovascularization by up-regulation of CXCR4 and CXCR7 expression in choroid endothelial cell. *PLoS One* 2015;10(8):e0136175.

19 Wang B, Wang W, Niu W, Liu E, Liu X, Wang J, Peng C, Liu S, Xu L, Wang L, Niu J. SDF-1/CXCR4 axis promotes directional migration of colorectal cancer cells through upregulation of integrin alphavbeta6. *Carcinogenesis* 2014;35(2):282-291.

20 Friedlander M, Theesfeld CL, Sugita M, Fruttiger M, Thomas MA, Chang S, Cheresh DA. Involvement of integrins alpha v beta 3 and alpha v beta 5 in ocular neovascular diseases. *Proc Natl Acad Sci U S A* 1996;93(18):9764-9769.

21 Reynolds LE, Wyder L, Lively JC, Taverna D, Robinson SD, Huang X, Sheppard D, Hynes RO, Hodivaladilke KM. Enhanced pathological angiogenesis in mice lacking beta3 integrin or beta3 and beta5 integrins. *Nature Medicine* 2002;8(1):27-34.

22 Jones J, Marian D, Weich E, Engl T, Wedel S, Relja B, Jonas D, Blaheta RA. CXCR4 chemokine receptor engagement modifies integrin dependent adhesion of renal carcinoma cells. *Exp Cell Res* 2007;313(19):4051-4065.